PROD. TYPE: COM
PP: 1-13 (col.fig.: nil)

JQSRT2082 DTD VER: 5.0.1

ED: Prathiba
PAGN: Thanuja – SCAN: Megha

ARTICLE IN PRESS

ELSEVIER

Journal of Quantitative Spectroscopy & Radiative Transfer ▮▮▮ (▮▮▮▮) ▮▮▮–▮▮▮

Journal of Quantitative Spectroscopy & Radiative Transfer

www.elsevier.com/locate/jqsrt

Global two-channel AVHRR aerosol climatology: effects of stratospheric aerosols and preliminary comparisons with MODIS and MISR retrievals

Igor V. Geogdzhayev[a, b], Michael I. Mishchenko[b, *], Li Liu[b, c], Lorraine Remer[d]

[a] *Department of Applied Physics and Applied Mathematics, Columbia University, 2880 Broadway, New York, NY 10025, USA*
[b] *NASA Goddard Institute for Space Studies, 2880 Broadway, New York, NY 10025, USA*
[c] *Department of Earth and Environmental Sciences, Columbia University, 2880 Broadway, New York, NY 10025, USA*
[d] *NASA Goddard Space Flight Center, Code 913, Greenbelt, MD 20771, USA*

Received 15 November 2003; accepted 15 March 2004

UNCORRECTED PROOF

Abstract

We present an update on the status of the global climatology of the aerosol column optical thickness and Ångström exponent derived from channel-1 and -2 radiances of the advanced very high resolution radiometer (AVHRR) in the framework of the Global Aerosol Climatology Project (GACP). The latest version of the climatology covers the period from July 1983 to September 2001 and is based on an adjusted value of the diffuse component of the ocean reflectance as derived from extensive comparisons with ship sun-photometer data. We use the updated GACP climatology and stratospheric aerosol and gas experiment (SAGE) data to analyze how stratospheric aerosols from major volcanic eruptions can affect the GACP aerosol product. One possible retrieval strategy based on the AVHRR channel-1 and -2 data alone is to infer both the stratospheric and the tropospheric aerosol optical thickness while assuming fixed microphysical models for both aerosol components. The second approach is to use the SAGE stratospheric aerosol data in order to constrain the AVHRR retrieval algorithm. We demonstrate that the second approach yields a consistent long-term record of the tropospheric aerosol optical thickness and Ångström exponent. Preliminary comparisons of the GACP aerosol product with MODerate resolution Imaging Spectrometer (MODIS) and multiangle imaging spectro-radiometer aerosol retrievals show reasonable agreement, the GACP global monthly optical thickness being lower than the MODIS one by approximately 0.03. Larger differences are observed on a regional scale. Comparisons of the GACP and MODIS Ångström exponent records are less conclusive and require further analysis.
© 2004 Published by Elsevier Ltd.

Keywords: Atmospheric aerosols; Optical thickness; Remote sensing

* Corresponding author. Tel.: +1-212-678-5590; fax: +1-212-678-5622
E-mail address: crmim@giss.nasa.gov mmishchenko@giss.nasa.gov (M.I. Mishchenko).

0022-4073/$ - see front matter © 2004 Published by Elsevier Ltd.
doi:10.1016/j.jqsrt.2004.03.024

1. Introduction

The totality of recent research results provides a strong indication that tropospheric aerosols have a significant impact on climate by both directly modulating the solar radiative fluxes and altering the radiative properties of clouds [1–3]. However, the magnitude of this impact and the human contribution to its temporal variation remain highly uncertain due to the complex and variable nature of aerosol properties.

Advanced very high resolution radiometer (AVHRR) instruments on board of National Atmospheric and Oceanic Administration (NOAA) weather satellites are a unique source of information about aerosol properties due to the extensive length of their combined data record and the global coverage. Having this in mind, we have developed an algorithm to retrieve the aerosol optical thickness (AOT), τ, and Ångström exponent, A, from AVHRR channel-1 and -2 radiances in the framework of the Global Aerosol Climatology Project (GACP) [4]. The latter was established jointly by the National Aeronautics and Space Administration (NASA) and the World Climate Research Programme's Global Energy and Water Cycle Experiment (GEWEX).

The goal of this paper is to provide an update on the status of the GACP data product. In the following section, we will describe an improved version of the retrieval algorithm, which incorporates changes suggested by the results of extensive comparisons of satellite retrievals and ship-borne sun-photometer observations [5], and present the latest version of the aerosol climatology covering the period from July 1983 to September 2001. In Section 3, we analyze the potential influence of volcanic aerosols on the GACP aerosol record by using stratospheric aerosol and gas experiment (SAGE) data and two different retrieval strategies. Finally, we take advantage of the availability of contemporaneous AVHRR, MODerate resolution Imaging Spectrometer (MODIS), and multiangle imaging spectro-radiometer (MISR) observations and present the results of a preliminary comparison of the GACP retrieval results with those derived from the more advanced satellite data.

2. Updated GACP climatology

Mishchenko et al. [6] published an AVHRR-derived climatology of the tropospheric AOT and Ångström exponent for a period extending through December 1999. Liu et al. [5] have since used ship-borne sun-photometer observations with well-characterized accuracy to validate the two-channel AVHRR aerosol retrievals and concluded that the satellite-derived AOT values are in good agreement with the sun-photometer data. Furthermore, they have found that by adjusting the diffuse component of the ocean surface reflectance from 0.002 to 0.004 in AVHRR channels 1 and 2, it is possible to reduce a residual positive offset observed in the satellite retrievals with respect to the sun-photometer data. Since the ocean surface reflectance is variable, the number Li et al. were aiming for was one that gave as good an average AOT result as possible with a single value.

We have, therefore, recalculated the entire GACP data set by using the new ocean diffuse reflectance value 0.004 and have extended the GACP record through September 2001 (the end of the lifetime of the NOAA-14 AVHRR). The resulting product is posted on the world wide web at http://gacp.giss.nasa.gov/retrievals and is illustrated in Fig. 1. The upper panel shows the global monthly mean AOT values (solid curve) as well as corresponding averages over the Southern (dotted curve) and Northern (dashed curve) Hemispheres. The lower panel depicts the respective monthly averages of the Ångström exponent. One

UNCORRECTED PROOF

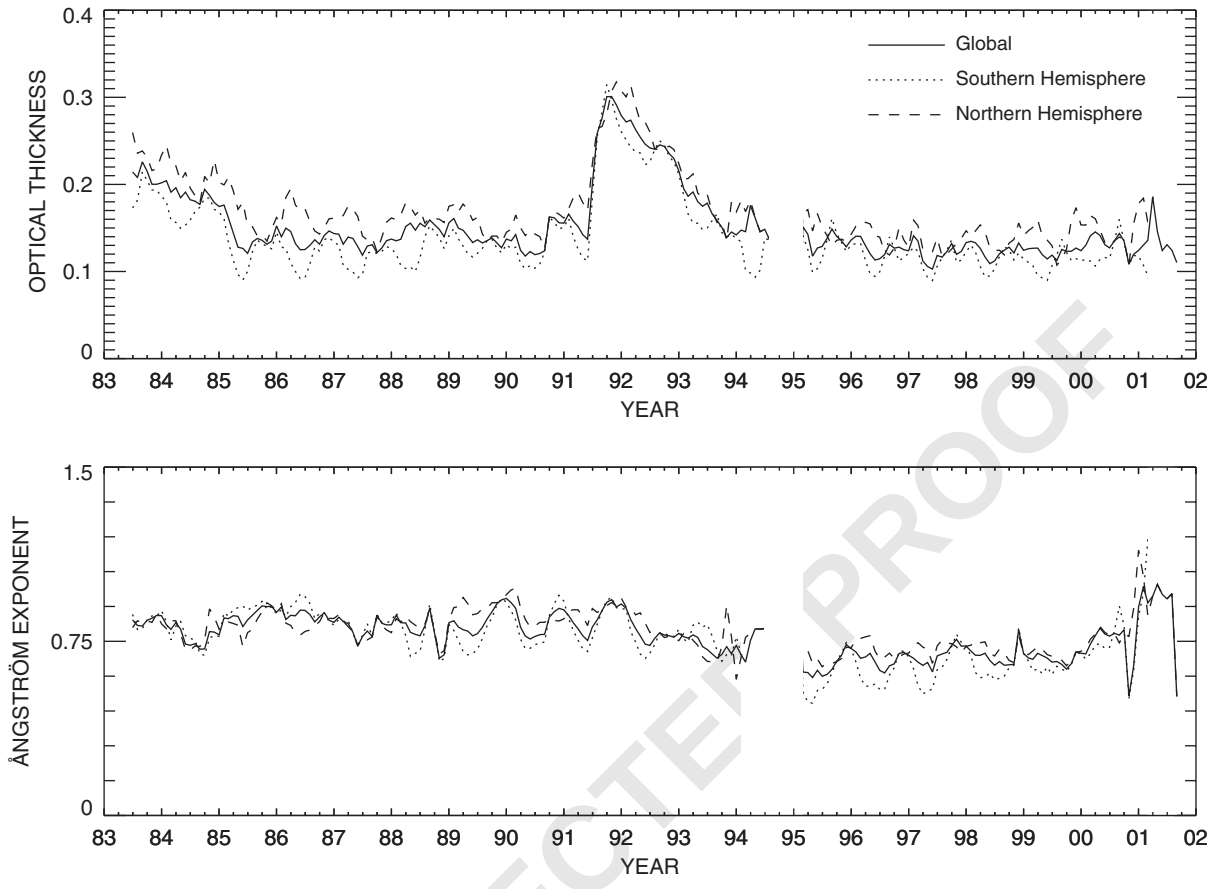

Fig. 1. Time series of the global monthly mean AOT and Ångström exponent retrieved from the AVHRR channel-1 and -2 data.

UNCORRECTED PROOF

can see that the main features of the global aerosol record discussed in [6] are preserved in the updated climatology, so that the previously reached conclusions about seasonal trends and hemisphere differences remain unchanged. One noticeable consequence of increasing the diffuse surface reflectance value is a reduction of the long-term global aerosol optical thickness from the previous value 0.145 [6] to 0.13. The global value of the Ångström exponent has not changed much from the old value 0.75 [6]. The extension of the record through September 2001 does not reveal any new trends in the AOT. The sharp oscillations of the Ångström exponent observed in late 2000 and through 2001 may be explained by poor data quality at the end of the AVHRR instrument lifetime as well as by the significant drift of the satellite orbit that made unavailable AVHRR data for the Southern Hemisphere after March 2001. Since the NOAA-16/L satellite was launched in September 2000, there is a significant overlap in the NOAA-14 and -16 AVHRR data records. We therefore, expect to be able to improve the quality of the GACP retrievals and to rectify these problems once the new AVHRR data have been calibrated and processed.

3. Effects of stratospheric aerosols on the AVHRR climatology

The long-term GACP record (Fig. 1) indicates that stratospheric aerosols had a strong impact on the column AOT after the El Chichon (March 1982) and Mt. Pinatubo (June 1991) eruptions. The former manifests itself as increased AOT values at the beginning of the GACP data record from July 1983 through the middle of 1985. The latter resulted in a sharp increase in the global AOT in the second half of 1991 with the peak value being twice as big as the background value, followed by a gradual decrease to the background level by 1995. The remarkable prominence of these events makes it very important to analyze the effect of volcanic aerosols on the performance of the GACP retrieval algorithm and on the resulting aerosol product.

It is widely recognized that the SAGE data are a unique source of information about stratospheric aerosols [7]. Mishchenko et al. [6] have used these data to develop a simple adjustment procedure for the NOAA-11 aerosol retrievals in order to solve an apparent calibration problem that manifested itself as a discontinuity in the AOT record at the time of transition from NOAA-9 to NOAA-11 as well as artificial trends in the AOT and Ångström exponent records. Their approach was to subtract the SAGE optical thickness from the total monthly mean AVHRR AOT, thereby creating a proxy for the tropospheric AOT. This proxy is relatively insensitive to the presence of volcanic aerosols and was subsequently used to compare the NOAA-9, -11, and -14 retrievals and to develop a correction to the NOAA-11 channel-2 calibration offset in such a way that the continuity of the tropospheric AOT record was restored and the artificial trends in the AOT and Ångström exponent records were removed.

However, one may expect that this approach gives only an approximate value of the tropospheric AOT during the periods affected by the El Chichon and Mt. Pinatubo eruptions and that a potentially more accurate estimate could be obtained by explicitly modeling the stratospheric aerosol layer in the GACP inversions. Although the radiative transfer scheme that we use for the computation of the GACP look-up tables is quite flexible and allows an easy inclusion of a layer of stratospheric aerosols, the presence of an additional layer of particles with microphysics different from that of the tropospheric aerosols adds several more unknown model parameters and makes the already ill-posed inverse problem even worse. With only two pieces of measurement data (AVHRR channel-1 and -2 radiances) per pixel available, one can hope to retrieve only two model parameters. Therefore, there is a significant degree of arbitrariness in how to select these two parameters while keeping the rest of the model parameters fixed in space and time.

Within this limited framework, one may consider two distinct approaches. The first one is to fix the size distributions and refractive indices of the stratospheric and tropospheric aerosols and the altitude of the stratospheric aerosol layer and to retrieve the optical thicknesses of both layers. The advantage of this approach would be the ability to compare the AVHRR- and SAGE-retrieved stratospheric AOTs.

The second approach is to rely on the SAGE stratospheric AOT and to retrieve the optical thickness and size of the tropospheric aerosols. The obvious advantage of the second approach is that it would enable one to verify the expected long-term constancy of the global annual means of the tropospheric aerosol parameters.

Below we analyze these two approaches in more detail and describe their application to the development of the long-term GACP record.

UNCORRECTED PROOF

3.1. Approach 1

Two fixed microphysical models of the stratospheric and tropospheric aerosols were considered. For the tropospheric aerosol, we used a model based on a power-law size distribution and a refractive index of 1.5+0.003i. This model is equivalent to the one used in the operational GACP algorithm but with a power-law exponent fixed at 3.8. This value was chosen because it yields the Ångström exponent value of 0.75, which is close to the previously obtained long-term global mean value [6]. The stratospheric aerosol was assumed to be nonabsorbing and was characterized by the refractive index 1.44 and a gamma size distribution [8] with the effective radius $r_{\text{eff}} = 0.45$ μm and the effective variance $v_{\text{eff}} = 0.35$. The effective radius value was chosen based on the SAGE data as being representative of the periods of high stratospheric aerosol loads after the Mt. Pinatubo eruption. Although nonabsorbing particles are typical of the background stratospheric aerosol and may not be an adequate model of fresh volcanic aerosol, the model of nonabsorbing aerosol seems to be a rational zero-order approximation given the necessity to select a fixed global value, as explained above. The vertical stratospheric-aerosol profile was modeled to follow that of ozone, while the tropospheric aerosols were assumed to be distributed vertically according to the vertical water vapor content.

Using this atmospheric model, a set of two look-up tables was generated for inverting the channel-1 and -2 AVHRR radiances, in which the tropospheric and stratospheric-aerosol optical thicknesses varied from 0 to 1.0 and from 0 to 0.3, respectively. We then attempted to retrieve simultaneously the tropospheric and the stratospheric AOT by seeking a minimum discrepancy between the measured and the calculated radiance values.

Test runs involving periods of low and high stratospheric aerosol loads demonstrated that the AVHRR-derived global average of the retrieved stratospheric AOT differed from the SAGE-retrieved results quite significantly. A subsequent detailed analysis of the retrieval process has revealed a degeneracy, which is illustrated in Fig. 2 by plotting the error function

$$F_{\text{err}}(R_1, R_2) = \sqrt{\frac{(R_1 - R_{1\text{mes}})^2 + (R_2 - R_{2\text{mes}})^2}{R_{1\text{mes}}^2 + R_{2\text{mes}}^2}} \tag{1}$$

for a particular viewing geometry as a function of the tropospheric and stratospheric-aerosol optical thicknesses, where R_1 and R_2 are the calculated and $R_{1\text{mes}}$ and $R_{2\text{mes}}$ are the measured radiances, respectively, in AVHRR channels 1 and 2. This specific plot refers to the measurement performed on 2 July 1992 for the pixel with coordinates 58.3°N and 152°W. The corresponding solar zenith angle, satellite zenith angle, and the satellite–sun azimuth angle difference were 47.2°, 40.6°, and 158.0°, respectively, while the measured channel-1 and -2 reflectances were $R_1 = 0.048$ and $R_2 = 0.026$, respectively. In addition, the dashed and dot-dashed lines show the contours of theoretical channel-1 and -2 radiances in the $(\tau_{\text{trop}}, \tau_{\text{strat}})$ parameter space at the levels corresponding to the measured values. One can see that the discrepancy between the measured and the calculated reflectances is minimized by an essentially infinite number of couplets $(\tau_{\text{trop}}, \tau_{\text{strat}})$ such that $\tau_{\text{trop}} + \tau_{\text{strat}} \approx 0.23$. This obviously suggests that it is impossible to simultaneously retrieve the tropospheric and stratospheric AOTs from the AVHRR channel-1 and -2 radiances. Instead, the specific selection of the couplet $(\tau_{\text{trop}}, \tau_{\text{strat}})$ by the retrieval algorithm is controlled by the instrumental noise and numerical errors and is random rather than deterministic. Quite similar patterns emerge when one considers other viewing geometries and measured radiance values.

UNCORRECTED PROOF

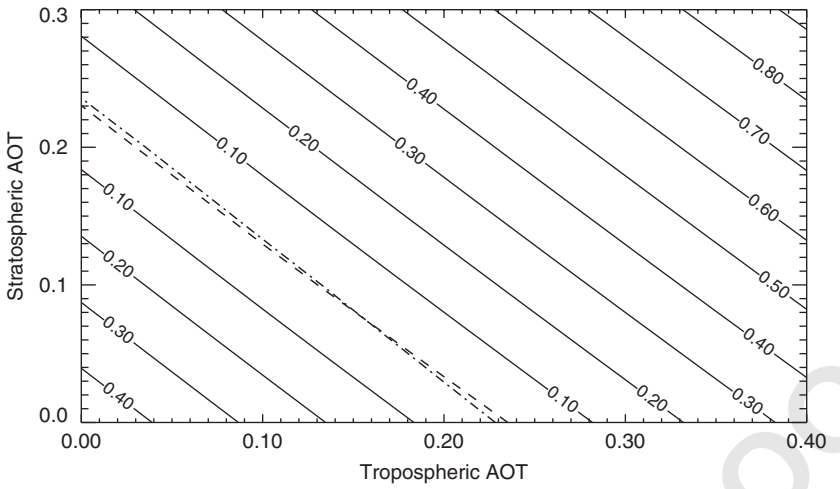

Fig. 2. Error function defined by Eq. (1) as a function of the tropospheric and stratospheric AOTs (see text).

The physical explanation of this behavior is that the spectral properties of the stratospheric and tropospheric aerosols are not sufficiently different to allow an effective separation of the two fractions based on the reflected radiances in the two closely spaced broadband AVHRR channels. Note that the problem is mostly caused by the physical limitations imposed by the specific configuration of AVHRR channels 1 and 2 rather than by measurement and/or numerical errors. This situation may be contrasted to the operational GACP retrieval algorithm, in which the two model variables (the total AOT and the Ångström exponent) are nearly "orthogonal," thereby enabling one to retrieve them separately [4].

Thus we have to conclude that one cannot retrieve the stratospheric AOT separately from the tropospheric AOT from the AVHRR radiance data alone. Therefore, the former must be inferred independently from another data set (e.g., from the SAGE data) or derived from aerosol transport-chemistry models.

3.2. Approach 2

The second approach we implemented is based on using the SAGE-retrieved stratospheric AOT and size in order to infer the tropospheric AOT and Ångström exponent from the AVHRR data. Since the SAGE data are relatively sparse compared to the AVHRR data and are not collocated, we decided to use time and space averages of the SAGE results in the AVHRR retrievals. Specifically, we selected the data set developed by Hansen et al. [7], which consists of monthly zonal means of the stratospheric AOT and effective radius r_{eff}. A straightforward inclusion of this auxiliary information in the GACP algorithm would require the addition of two extra dimensions (the stratospheric AOT and effective radius) to the channel-1 and -2 look-up tables. However, the effect of r_{eff} is only important when the stratospheric aerosol load is high (i.e., shortly after a volcanic eruption), whereas during normal (clean) periods the uncertainty associated with its variability is negligible since the contribution of the background stratospheric aerosol to the top-of-the-atmosphere radiance is minor compared to that of the tropospheric aerosol. We therefore

UNCORRECTED PROOF

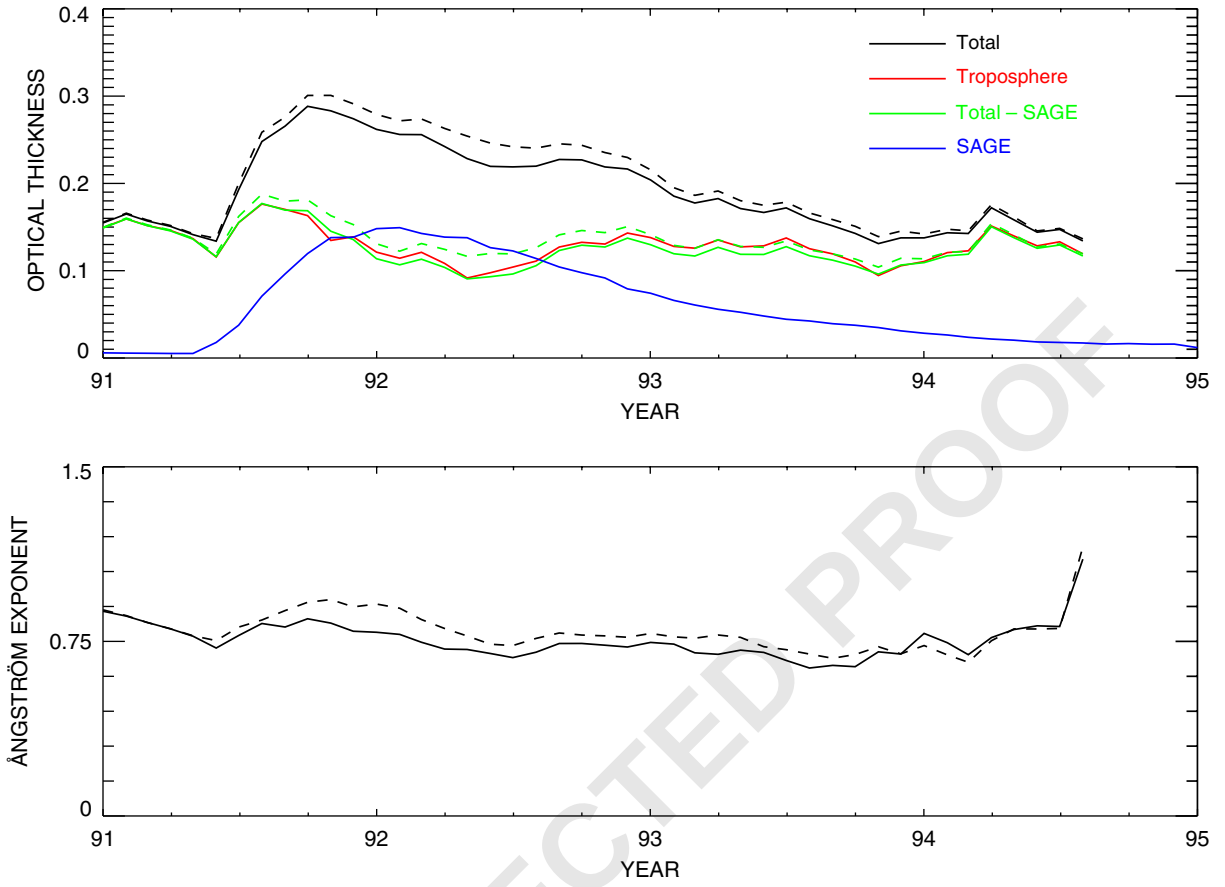

Fig. 3. Time series of the global monthly mean AOT and Ångström exponent retrieved from the AVHRR data and the global monthly mean optical thickness of stratospheric aerosols retrieved from the SAGE data (see text).

UNCORRECTED PROOF

decided to model the stratospheric aerosol using the fixed value $r_{\text{eff}} = 0.45$ μm, as rationalized in the previous subsection, thereby adding only one extra dimension to our look-up tables.

The algorithm was applied to the time period extending from 1991 to 1995, which was affected by the Mt. Pinatubo eruption. The results are shown in Fig. 3, in which solid curves depict the quantities retrieved using the second approach and dashed curves show the corresponding quantities retrieved with the operational GACP algorithm. The black curves show the total global monthly mean AOT (the upper panel) and Ångström exponent (the lower panel). The green curves depict the difference of the total AOT and the SAGE-retrieved stratospheric AOT. The red curve corresponds to the AVHRR-retrieved tropospheric AOT. Also shown is the SAGE stratospheric AOT (the blue curve).

One can see that both the simple subtraction of the SAGE AOT from the total AOT (the solid green curve) and the actual retrieval of the tropospheric AOT (the red curve) help to eliminate the volcanic effect from the long-term record and give very close results. The residual increase in the tropospheric AOT observed shortly after the eruption can be explained by the fact that the vertical distribution of the

volcanic aerosol was sufficiently uniform at that time and contributed both to the tropospheric AOT and the stratospheric AOT measured by SAGE. In addition, the optical properties of the fresh volcanic aerosol may have been significantly different from the aerosol model assumed in the retrieval algorithm. The total AOT is slightly lower at the time of maximum aerosol load compared with that retrieved with the operational GACP algorithm. This is mainly due to the nonabsorbing stratospheric aerosol model used and the fact that the stratospheric aerosol was located above most of the absorbing atmospheric water vapor, thereby appearing brighter. The retrieved Ångström exponent is similar to that yielded by the operational algorithm with largest differences occurring during the period of maximum aerosol loads, as expected. The tropospheric aerosol record exhibits no discernable trends and is in good overall agreement with that during the periods not affected by volcanic aerosols.

4. Preliminary comparisons with MODIS and MISR aerosol retrievals

The GACP data set has been used in a number of recent validation and intercomparison studies [5,10–14]. They have included comparisons with ground- and air-borne data [5,10,14] and models [11,12] as well as with data sets obtained from other satellite sensors and algorithms [12,15–19]. The results of these studies both increase our confidence in the robustness of the GACP aerosol climatology and help to understand its limitations. Geogdzhayev et al. [14] have concluded that one of the most promising approaches to validating the GACP retrievals is to compare them with the newer and more advanced satellite products such as the MODIS and MISR aerosol records. These newer instruments have some ability to account for particle property variations that affect AOT retrievals. They also have advantages in spatial resolution (which may improve cloud clearing), in sensitivity (with the help of additional spectral bands or angles), and possibly in radiometric calibration. As such, regional differences between the AVHRR and the MODIS and MISR products will be of great interest, since they will test the limits of assuming a single particle type globally, as well as differences in cloud clearing, etc.

The extension of the GACP record through September 2001 allowed us for the first time to directly compare our retrievals with those derived from the MODIS and MISR radiance data. For this purpose, we have used the MODIS Level 3 monthly mean AOT values at 550 nm and the Ångström exponent values calculated from the AOT values in two channels [19]. The spatial resolution of the MODIS Level 3 data is $1^\circ \times 1^\circ$. Also, we have used the MISR Level 3 monthly AOT data at 555 nm with the $0.5^\circ \times 0.5^\circ$ spatial resolution [21]. Only the retrievals over the oceans have been included.

Fig. 4 compares the MODIS, MISR, and GACP global monthly mean AOTs (the upper panel) and the MODIS and GACP global mean Ångström exponents (the bottom panel). MISR Level 3 Ångström exponent data were not available at the time of this publication and are not shown. One can see a generally reasonable agreement between the AVHRR- and MODIS-retrieved AOT values. The MODIS AOTs are systematically higher than the GACP AOTs by about 0.03 and systematically lower than the MISR AOTs by approximately the same amount. The three curves correlate well, which is encouraging given the somewhat different spatial coverage afforded by these instruments. It also gives us confidence that the orbital shift at the end of the NOAA-14 operation and the associated change in the AVHRR spatial coverage did not distort significantly the retrieved global monthly mean AOT values. Note that although the MODIS and MISR global averages were calculated by including all pixels, the inclusion of only those pixels for which the contemporaneous AVHRR data were available does not change the results significantly.

UNCORRECTED PROOF

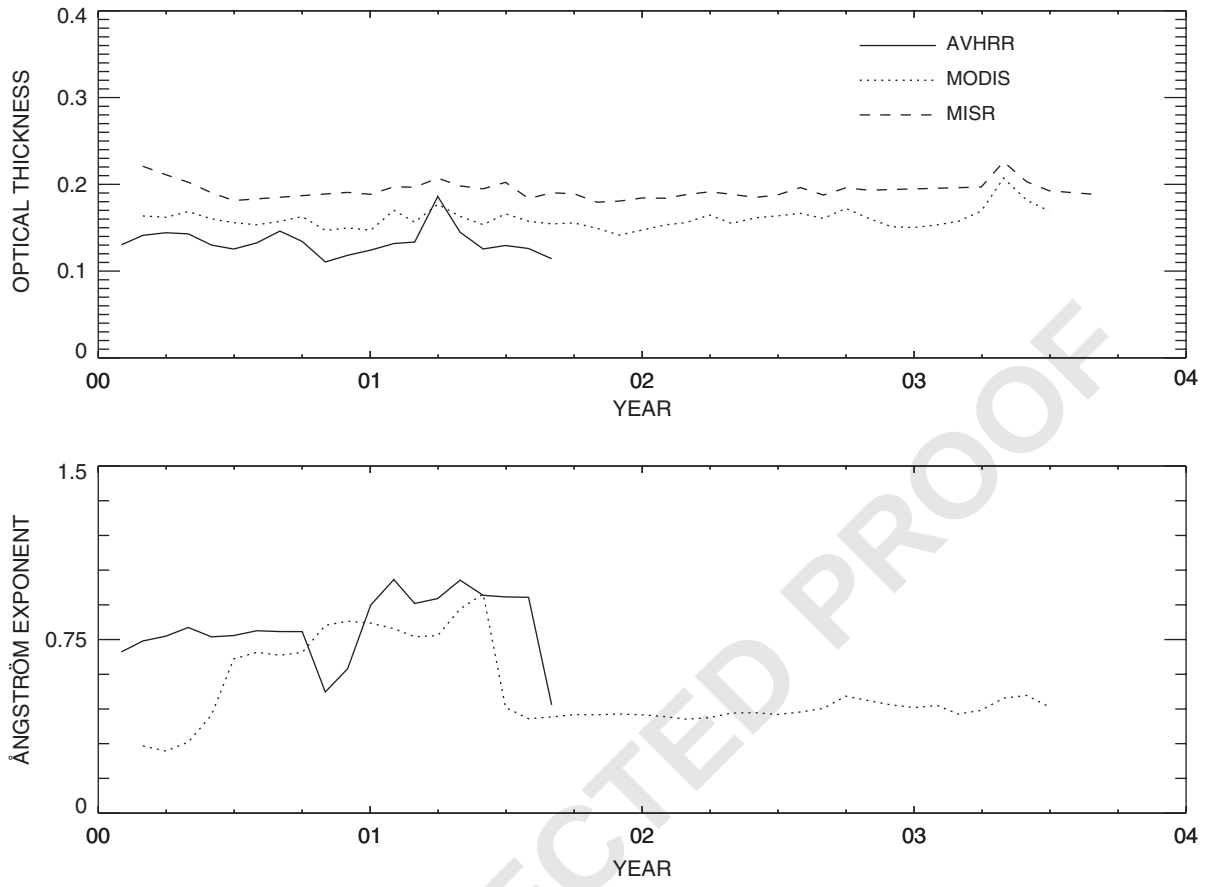

Fig. 4. Time series of the global monthly mean AOT and Ångström exponent retrieved from the AVHRR, MODIS, and MISR radiance data.

UNCORRECTED PROOF

The comparison of the Ångström exponent records reveals large fluctuations in both the AVHRR and the MODIS results. While an abrupt change in the AVHRR-retrieved values at the end of the record is associated with the orbital shift and general deterioration of the quality of the AVHRR radiance data, the cause of the large changes in the MODIS record is not clear. High values of the Ångström exponent in the extreme polar regions have certainly contributed to the higher values at the beginning of the record. However, limiting the comparison to the MODIS data collected at latitudes lower than $\pm 60°$ still produces large fluctuations in the Ångström exponent. It should also be noticed that the GACP aerosol model assumes a wavelength-independent Ångström exponent, whereas the MODIS retrieval algorithm calculates the Ångström exponent from the ratio of AOTs in two channels and generally depends on wavelength. Obviously, further analysis of the Ångström exponent records is necessary.

Given the good correlation of the global AOT record, it is interesting to see what happens on the regional scale. In fact, one might expect to observe significant differences based on the fact that the GACP retrievals are performed using a single globally fixed model of all aerosol properties except the Ångström exponent,

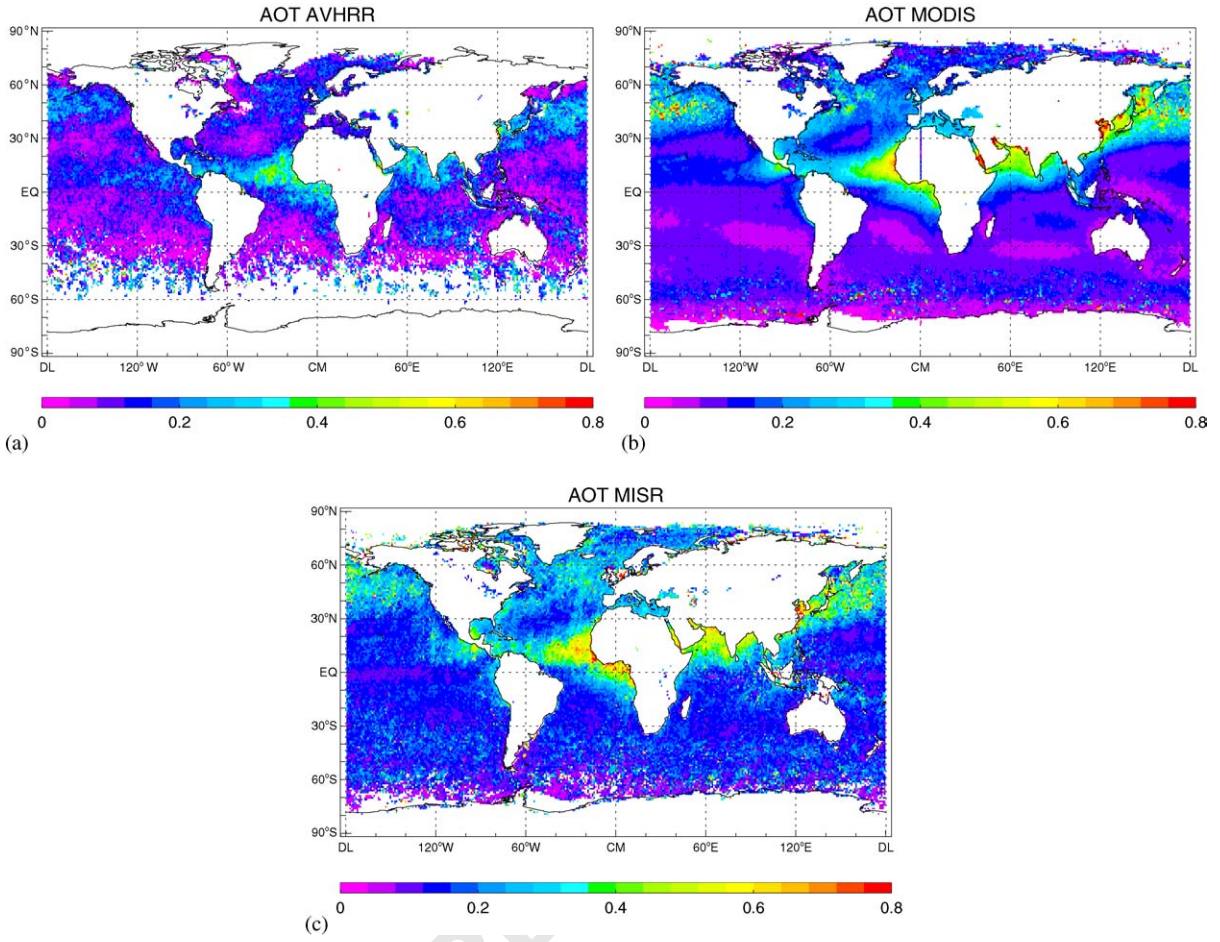

Fig. 5. Monthly averages of the AOT for the period from March to July 2000 compiled from (a) the two-channel AVHRR retrievals, (b) the MODIS aerosol data, and (c) the MISR aerosol data.

whereas the advanced capabilities of the MODIS and MISR instruments allow for more sophisticated retrieval algorithms using sets of aerosol models with varying optical properties [19,20].

Fig. 5 shows maps of the GACP, MODIS, and MISR AOT values averaged over the period from March to July of 2000. One can see that the MODIS and MISR data extend further towards the poles than the AVHRR data. This is especially noticeable at mid latitudes of the Southern Hemisphere where the AVHRR results are patchy due to the orbital drift and appear to be "noisy" because of a smaller number of individual retrievals contributing to each $1^\circ \times 1^\circ$ pixel. The general structure of the global aerosol fields retrieved by all three satellites is remarkably similar, with local minima and maxima occurring in exactly the same regions. For example, the dust outflows from the Sahara desert, Persian Gulf, and Far East and a belt of elevated AOT values in the Southern Hemisphere are all present in the same locations. However, the magnitude of these features differs between the instruments. The AVHRR retrievals tend to

produce smaller values in areas with high aerosol loads and somewhat smaller values for the background aerosols in open ocean areas. The MISR retrievals are similar to the MODIS results in the areas with high aerosol loads and are significantly higher than the AVHRR- and MODIS-retrieved AOTs in the open ocean areas. The belt of higher aerosol loads in the Southern Hemisphere is probably associated with sea salt particles and is more pronounced in the AVHRR than in the MODIS results, although the lack of detailed contemporaneous AVHRR data in that area does not allow us to make a definitive judgment.

Several possible explanations can be suggested for the observed discrepancies. First, differences in the cloud screening algorithms may have been significant contributors, especially in the Southern Hemisphere. Second, our retrieval algorithm may not always distinguish between optically thick aerosols and clouds [4], which may be a significant source of differences in areas with high aerosol loads. One may also suspect that while the aerosol model used in the AVHRR retrievals can be expected to perform reasonably well globally, it may not be the best choice in the areas affected by optically thick dust plumes.

It is also anticipated that the preliminary MODIS and MISR aerosol products will become significantly better in the near future. Indeed, the currently available MISR aerosol product is not yet fully validated. The expected refinements to the MISR calibration, particle models used in the retrieval, and possibly treatment of the ocean surface boundary condition, will affect the results. For example, a correction to the MISR band-to-band radiometric calibration reduces the AOT retrieved over a broad sampling of dark water sites by about 0.025 (Kahn et al.), thereby reducing the discrepancy with sun-photometer (and apparently with AVHRR) values by 40%.

In any case, this comparison is only a very preliminary step in what should be a sustained and significant effort. We hope that the extension of the GACP record using the NOAA-16 data as well as a more detailed analysis approach will help us to better quantify the differences between the various aerosol products and to understand their potential causes.

5. Conclusions

We have presented an updated global long-term (July 1983–September 2001) climatology of aerosol optical thickness and Ångström exponent derived from AVHRR channel-1 and -2 radiance measurements. This climatology incorporates an adjusted value of the diffuse component of the ocean surface reflectance in order to provide a better agreement with extensive ship-borne sun-photometer data. The updated GACP record preserves the main features of the time series reported in our previous publications, but implies a slight reduction of the global mean AOT from 0.145 to 0.13. We expect that problems associated with the orbital drift and data quality deterioration at the end of the NOAA-14 lifetime will be ameliorated once the contemporaneous data from the NOAA-16 AVHRR are processed.

We have analyzed two ways of treating stratospheric aerosols in the two-channel AVHRR retrieval algorithm during the periods affected by major volcanic eruptions. It has been shown that one cannot retrieve the stratospheric and the tropospheric AOT simultaneously using AVHRR channel-1 and -2 radiances because of the insufficient difference between the spectral effects caused by the two aerosol fractions. However, we have demonstrated that the auxiliary data on the stratospheric AOT and size provided by SAGE can be incorporated in the AVHRR retrieval algorithm in order to obtain a continuous long-term global record of the tropospheric AOT and Ångström exponent.

Preliminary comparisons with the MODIS and MISR aerosol results have revealed a reasonable correlation between the global monthly averages of the AOT records during the period when contemporaneous

UNCORRECTED PROOF

AVHRR data were available (March 2000–September 2001), the GACP retrievals being systematically lower than the MODIS and MISR results by approximately 0.03 and 0.06, respectively. The comparison of the GACP and MODIS Ångström exponent results is less conclusive and requires further analysis.

Regional comparisons show that the GACP algorithm retrieves smaller AOT values in the areas affected by desert dust aerosols compared to the MODIS and MISR results. This may be due to the potentially imperfect differentiation between clouds and optically thick aerosols by the operational GACP algorithm, as discussed above, and/or due to a bias associated with the globally fixed aerosol model. The significant differences in the GACP, MODIS, and MISR cloud screening approaches may also have contributed to the differences in the aerosol retrieval results, especially at mid latitudes in the Southern Hemisphere, where high sea salt concentrations may be expected to be the cause of greater AOT values.

We expect that further extension of the GACP record using NOAA-16 data will help us to arrive at more quantitative and more definitive conclusions.

6. Uncited references

[9]

Acknowledgements

We thank Ralph Kahn and two anonymous reviewers for valuable advice and helpful suggestions. The MODIS and MISR data used in this study were obtained from the NASA Langley Research Center Atmospheric Sciences Data Center. This research was supported by the NASA Radiation Sciences Program managed by Donald Anderson.

References

[1] Hansen JE, Sato M, Lacis A, Ruedy R, Tegen I, Matthews E. Perspective: climate forcings in the industrial era. Proc Natl Acad Sci 1998;95:12753–8.
[2] Kaufman YJ, Tanré D, Gordon HR, Nakajima T. Passive remote sensing of tropospheric aerosol and atmospheric corrections of the aerosol effect. J Geophys Res 1997;102:16815–7217 (special issue).
[3] Mishchenko M, Penner J, Anderson D. Global aerosol climatology project. J Atmos Sci 2002;59:249–783.
[4] Mishchenko MI, Geogdzhayev IV, Cairns B, Rossow WB, Lacis AA. Aerosol retrievals over the ocean by use of channels 1 and 2 AVHRR data: sensitivity analysis and preliminary results. Appl Opt 1999;38:7325–41.
[5] Liu L, Mishchenko MI, Geogdzhayev I, Smirnov A, Sakerin SM, Kabanov DM, Ershov OA. Global validation of two-channel AVHRR aerosol optical thickness retrievals over the oceans. JQSRT 2004; (this issue).
[6] Mishchenko MI, Geogdzhayev IV, Liu L, Ogren JA, Lacis AA, Rossow WB, Hovenier JW, Volten H, Muñoz O. Aerosol retrievals from AVHRR radiances: effects of particle nonsphericity and absorption and an updated long-term global climatology of aerosol properties. JQSRT 2003;79/80:953–72.
[7] Hansen J, Sato M, Nazarenko L, Ruedy R, Lacis A, Koch D, Tegen I, Hall T, Shindell D, Stone P, Novakov T, Thomason L, Wang R, Wang Y, Jacob D, Hollandsworth S, Bishop L, Logan J, Thompson A, Solarski R, Lean J, Willson R, Levitus S, Antonov J, Rayner N, Parker D, Christy J. Climate forcings in GISS SI200 simulations. J Geophys Res 2002;107 (doi:10.1029/ 2001JD001143).
[8] Hansen JE, Travis LD. Light scattering in planetary atmospheres. Space Sci Rev 1974;16:527–610.
[9] Kinne S, Holben B, Eck T, Smirnov A, Dubovik O, Slutsker I, Tanré D, Zibozdi G, Lohmann U, Ghan S, Easter R, Chin M, Ginoux P, Takemura T, Tegen I, Koch D, Kahn R, Vermote E, Stowe L, Torres O, Mishchenko M, Geogdzhayev I,

UNCORRECTED PROOF

Higurashi A. How well do aerosol retrievals from satellites and representation in global circulation models match ground-based AERONET aerosol statistics. in: Beniston M, Verstraete MM., (editors.) Remote sensing and climate modeling: Synergies and limitations. Dordrecht: Kluwer Academic Publishers; 2001. pp. 103–58.

[10] Haywood JM, Francis PN, Geogdzhayev I, Mishchenko M, Frey R. Comparison of Saharan dust aerosol optical depths retrieved using aircraft mounted pyranometers and 2-channel AVHRR algorithms. Geophys Res Lett 2001;28:2393–6.

[11] Penner JE, Zhang SY, Chin M, Chuang CC, Feichter J, Feng Y, Geogdzhayev IV, Ginoux P, Herzog M, Higurashi A, Koch D, Land D, Lohmann U, Mishchenko M, Nakajima T, Pitari G, Soden B, Tegen I, Stowe L. A comparison of model-and satellite-derived aerosol optical depth and reflectivity. J Atmos Sci 2002;59:441–60.

[12] Yu H, Dickinson RE, Chin M, Kaufman YJ, Holben BN, Geogdzhayev IV, Mishchenko MI. Annual cycle of global distributions of aerosol optical depth from integration of MODIS retrievals and GOCART model simulations. J Geophys Res 2003;108 (doi:10.1029/ 2002JD002717).

[13] Myhre G, Stordal F, Johnsrud M, Ignatov A, Mishchenko MI, Geogdzhayev IV, Tanré D, Goloub P, Nakajima T, Higurashi A, Torres O, Holben BN. Intercomparison of satellite retrieved aerosol optical depth over ocean. J Atmos Sci 2004;12 (in press).

[14] Geogdzhayev IV, Mishchenko MI, Rossow WB, Cairns B, Lacis AA. Global two-channel AVHRR retrievals of aerosol properties over the ocean for the period of NOAA-9 observations and preliminary retrievals using NOAA-7 and NOAA-11 data. J Atmos Sci 2002;59:262–78.

[15] Ignatov A, Stowe L. Aerosol retrievals from individual AVHRR channels. I Retrieval algorithm and transition from Dave to 6S radiative transfer model. J Atmos Sci 2002;59:313–34.

[16] Torres O, Bhartia PK, Herman JR, Ahmad Z. Derivation of aerosol properties from satellite measurements of backscattered ultraviolet radiation. Theoretical basis. J Geophys Res 1998;103:17099–110.

[17] Nakajima T, Higurashi A. A use of two-channel radiances for an aeresol characterization from space. Geophys Res Lett 1998;25:3815–8.

[18] Goloub P, Tanré D, Deuzé JL, Herman M, Marchand A, Bréon FM. Validation of the first algorithm applied for deriving the aerosol properties over ocean using the POLDER/ADEOS measurements. IEEE Trans Geosci Remote Sensing 1999;37:1586–96.

[19] Tanré D, Kaufman YJ, Herman M, Mattoo S. Remote sensing of aerosol properties over oceans using the MODIS/EOS spectral radiances. J Geophys Res 1997;102:16971–88.

[20] Kahn R, Banerjee P, McDonald D. Sensitivity of multi-angle imaging to natural mixtures of aerosols over ocean. J Geophys Res 2001;106:18219–38.

[21] Lewicki S, Moroney C, Crean K, Gluck S, Miller K, Smyth M, Paradise S. MISR data product specifications. JPL D-13963. Revision J 2003.

UNCORRECTED PROOF